

# A Unifying View on Blind Source Separation of Convolutive Mixtures based on Independent Component Analysis

Andreas Brendel *Student Member, IEEE*, Thomas Haubner *Student Member, IEEE*,  
and Walter Kellermann *Fellow, IEEE*

**Abstract**—In many daily-life scenarios, acoustic sources recorded in an enclosure can only be observed with other interfering sources. Hence, convolutive Blind Source Separation (BSS) is a central problem in audio signal processing. Methods based on Independent Component Analysis (ICA) are especially important in this field as they require only few and weak assumptions and allow for blindness regarding the original source signals and the acoustic propagation path. Most of the currently used algorithms belong to one of the following three families: Frequency Domain ICA (FD-ICA), Independent Vector Analysis (IVA), and TRIPLeN Independent component analysis for CONvolutive mixtures (TRINICON). While the relation between ICA, FD-ICA and IVA becomes apparent due to their construction, the relation to TRINICON is not well established yet. This paper fills this gap by providing an in-depth treatment of the common building blocks of these algorithms and their differences, and thus provides a common framework for all considered algorithms.

**Index Terms**—Blind Source Separation, Independent Component Analysis, Convolutive Mixtures, Independent Vector Analysis, TRINICON

## I. INTRODUCTION

A real-world recording of an audio signal is often a mixture of the desired source and undesired signals, e.g., in a cocktail party scenario. When these recordings take place in acoustic enclosures, the observed microphone signals are affected by multiple reflections of the emitted signals, i.e., reverberation. Hence, the observed mixture is typically convolutive. Algorithms for convolutive BSS [1] aim at decomposing these mixtures into their individual source signals. “Blind” refers to the fact that no or only little prior knowledge about the mixing process or the source signals is exploited.

There exists a rich literature on convolutive BSS algorithms in the time domain as well as in the frequency domain including different separation principles and cost functions (see [2] for an overview of convolutive BSS methods). Here, we will focus on multichannel algorithms, i.e., on approaches that exploit spatial diversity.

A large class of convolutive BSS algorithms use the statistical properties of the source signals for separation. As

the main assumption is the statistical independence of the source signals, such algorithms are usually called Independent Component Analysis (ICA). These statistical approaches can roughly be divided into two main subclasses, Second-Order Statistics (SOS)- and Higher-Order Statistics (HOS)-based approaches. SOS-based approaches for separation of convolutive speech signal mixtures rely on the nonwhiteness [3] or the nonstationarity [4]–[6] of speech or audio signals or on both properties (see, e.g., [7] for an overview). HOS-based approaches use the assumption that the source signals are statistically independent, which can be expressed by 4th-order moments [8], [9], nonlinear cross-moments [10] or information theoretic measures, which are formulated w.r.t. the underlying source Probability Density Functions (PDFs) [11].

In this contribution, we concentrate on convolutive BSS methods based on ICA, as a representative of the last mentioned group of algorithms. The first works on ICA date back over thirty years, e.g., [11], and cover a broad variety of application scenarios including medical imaging, fMRI, EEG, telecommunications or stockmarket prediction [12].

However, ICA in its original form considers only instantaneous mixtures, which makes direct application to the separation of audio signals inappropriate in most cases, due to the dispersive multipath propagation of sound waves in enclosures. To address this issue, FD-ICA has been proposed, which models convolutive mixing by estimating demixing filters by instantaneous ICA for each frequency bin in the Short-Time Fourier Transform (STFT) domain [13]. However, then, the permutation ambiguity of ICA, i.e., the uncertainty about the order of the estimated signals at the outputs, appears in each frequency bin for FD-ICA. This yields the well-known inner permutation problem, which has to be resolved to obtain acceptable results [14].

To avoid the internal permutation problem, statistical coupling between the frequency bins of the demixed signals has been enforced within the class of IVA-based algorithms [15]. Fast and stable update rules based on the Majorize-Minimize (MM) principle have been proposed (auxIVA) [16] and a unification of IVA and Nonnegative Matrix Factorization (NMF) has been provided as the Independent Low-Rank Matrix Analysis (ILRMA) method [17]. For solving the external permutation problem, geometrically constrained IVA algorithms have been proposed [18]–[20] and a parametrization of the demixing matrices has been applied for signal extraction based on IVA in [21].

Andreas Brendel, Thomas Haubner and Walter Kellermann are with the chair of Multimedia Communications and Signal Processing, Friedrich-Alexander-Universität Erlangen-Nürnberg, Cauerstr. 7, D-91058 Erlangen, Germany, e-mail: {Andreas.Brendel, Thomas.Haubner, Walter.Kellermann}@FAU.de.

This work was partially funded by the Deutsche Forschungsgemeinschaft (DFG, German Research Foundation) – 282835863 – within the Research Unit FOR2457 “Acoustic Sensor Networks”.

TRINICON, a versatile framework for broadband adaptive Multiple Input Multiple Output (MIMO) processing modeling the nongaussianity, nonwhiteness and nonstationarity of signals like speech has been proposed in [22], [23] and provides a unified framework for SOS and HOS-based BSS approaches. TRINICON enables broadband acoustic BSS [24], estimation of the direction of arrival [25], signal extraction [26] and joint separation and dereverberation [27] and, as a broadband technique based on a time-domain cost function, inherently precludes the internal permutation problem. Further, the time-domain formulation ensures a linear convolution model for the demixing - corresponding to the convolutive mixing of the acoustic sources - instead of a circular convolution model as intrinsic to FD-ICA and IVA.

This paper provides a hitherto unavailable analytical, in-depth comparison of the three most popular ICA-based convolutive BSS approaches for audio signals, FD-ICA, IVA and TRINICON. While [24] provides a comparison of IVA and TRINICON for gradient-based updates, a comparison for the state-of-the-art optimization methods of IVA, e.g., MM-type update rules, and various versions of the gradient (holonomic or nonholonomic gradient) or Newton-type optimization strategies are still missing. Furthermore, a comparison of the update rules as in [24] does not explicitly show the underlying model assumptions. Therefore, a discussion of the differences of these approaches resulting from their different cost functions, which can be considered as the most general approach for comparing these methods, is provided in the sequel. We will establish a common basis for the derivation of these algorithms and highlight corresponding steps in their derivation. Especially the in-depth discussion of the relation of the IVA cost function to the TRINICON cost function is deemed beneficial as it shows that the TRINICON cost function contains the IVA cost function as a special case. Furthermore, we will provide an analysis of the demixing models underlying the considered approaches. Finally, IVA and TRINICON are compared by experiments using measured Room Impulse Responses (RIRs). Furthermore, benchmark results using oracle Relative Transfer Functions (RTFs) representing a linear or a circular convolution are provided.

The remainder of the paper is structured as follows: The assumed signal model is introduced in Section II. The cost functions of the three considered convolutive ICA-based BSS approaches FD-ICA, IVA and TRINICON are formulated in a unified manner in Sections III, IV and V, respectively. Thereby, we emphasize corresponding steps in the derivations of the cost functions to highlight similarities between the algorithms. In Section VI the relations between the algorithms are shown analytically. The identified differences are discussed in Section VII and experimental results quantifying the impact of the identified differences are presented. The paper is concluded in Section VIII.

## II. SIGNAL MODEL

### A. Notation

We introduce some notations and list the most important symbols in Tab. I for later reference. Scalar variables are

$\mathbf{I}, \mathbf{0}$	identity and all-zero matrix
$l$	time index
$N$	number of signal blocks
$n$	time frame index
$k$	frequency index
$K$	number of frequency bins, DFT length
$\mathbf{x}$	vector of microphone signals
$\mathbf{y}$	vector of demixed signals
$\mathbf{W}$	convolutive demixing matrix in time domain
$\underline{\mathbf{W}}$	instantaneous frequency bin-wise demixing matrix in STFT domain
$\underline{\mathbf{W}}$	IVA demixing matrix in STFT domain
$\underline{\mathbf{W}}$	extended demixing matrix in time domain
$p(\cdot)$	Probability Density Function (PDF)
$P$	number of source/microphone signals and output channels
$D, L$	parameters describing the signal lengths
$\mathbf{U}$	window matrix
$\underline{\mathbf{E}}_K$	DFT matrix for DFT length $K$
$\mathbf{P}$	permutation matrix
$\mathbf{C}_{\mathbf{W}_{pq}}$	circulant matrix corresponding to Toeplitz matrix $\mathbf{W}_{pq}$
$J$	cost function

TABLE I  
NOTATIONS USED

typeset as lower-case letters, constant scalars as upper-case letters, matrices as bold upper-case letters and vectors as bold lower-case letters. Underlined quantities ( $\underline{\cdot}$ ) denote STFT-domain variables. Subscripts of identity or all-zero matrices indicate their size, i.e.,  $(\cdot)_A$  indicates an  $A \times A$  matrix and  $(\cdot)_{A \times B}$  indicates a matrix of size  $A \times B$ . Superscripts of window matrices indicate their structure, i.e.,  $\mathbf{U}^{1,A,0}$  denotes an identity matrix of size  $A \times A$  stacked on top of an all-zero matrix.  $(\cdot)^T$  and  $(\cdot)^H$  denote transpose and Hermitian, respectively. Permuted matrices and vectors are marked with an overbar ( $\overline{\cdot}$ ). The expectation operator is denoted as  $\mathcal{E}\{\cdot\}$ , the Kullback-Leiber divergence as  $\mathcal{KL}\{\cdot\|\cdot\}$  and the differential entropy by  $\mathcal{H}(\cdot)$ .

### B. Convolution Model

In this contribution we consider a set of  $P$  acoustic point sources in a reverberant enclosure which are observed by  $P$  microphones, i.e., a determined scenario. Disregarding additive microphone noise, the  $p$ th microphone signal  $x_p(l)$  sampled at time instant  $l$  can be described in the discrete-time domain as a superposition of the convolutional products of the  $P$  acoustic sources with the corresponding RIRs<sup>1</sup>

$$x_p(l) = \sum_{q=1}^P \sum_{\kappa=0}^{N_{\text{RIR}}-1} h_{qp}(\kappa) s_q(l - \kappa), \quad (1)$$

where  $h_{qp}(\kappa)$ ,  $\kappa = 0, \dots, N_{\text{RIR}} - 1$  are the coefficients of the RIR from source  $q$  to microphone  $p$  and  $N_{\text{RIR}}$  is the number of Finite Impulse Response (FIR) filter coefficients, which are assumed to be time-invariant for the remainder of this paper.

The set of FIR models leading to the microphone observations is called the mixing system. A broad class of BSS algorithms aim at identifying a parametric demixing system, i.e., a set of FIR filters which estimates – potentially reverberated – versions of the original speech signals from the

<sup>1</sup>Note that a reasonable approximation of the RIRs can be obtained by a finite length  $N_{\text{RIR}}$ .

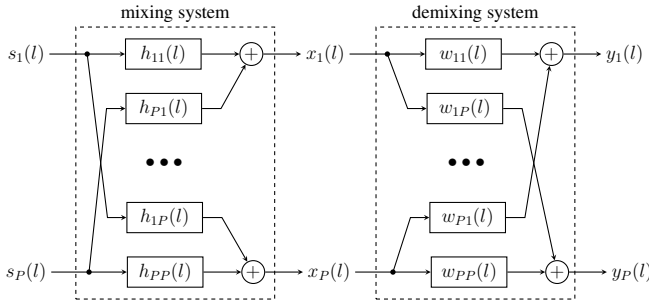


Fig. 1. Exemplary block diagram showing the mixing and demixing system for a scenario with  $P$  sources and  $P$  microphones.

observed mixture. The demixing system can be conveniently described by the so-called demixing matrix  $\mathbf{W}$  which is applied to the microphone signals to compute the demixed signals  $y_q(l)$  (see Fig. 1 for an illustration of the mixing and demixing systems). For generality and to cover both circular and linear convolution, the application of the demixing matrix  $\mathbf{W}$  is here abstracted by a function  $\text{conv}(\cdot)$  so that we can write the separated output signals  $y_q(l)$  as a function of the sensor signals  $x_p(l)$ ,  $p, q \in \{1, \dots, P\}$ , with filter length  $L$

$$[y_1(l), \dots, y_P(l)]^T = \text{conv}\left(\{x_1(l'), \dots, x_P(l')\}_{l+1-L \leq l' \leq l}\right). \quad (2)$$

As the mixing process is assumed to be time-invariant in this contribution, also the optimum demixing system to be identified can be assumed to be time-invariant here.

### III. FREQUENCY-DOMAIN INDEPENDENT COMPONENT ANALYSIS

A well-known approach to BSS of instantaneous mixtures is ICA [11]. In its original form [12], ICA is not directly applicable to convolutive mixtures captured by multiple sensors, due to the memory in the mixing system already caused by relative delays between the signals captured by different sensors. Therefore, the source separation problem is usually transformed into the STFT domain and ICA is applied in each frequency bin independently, which is commonly termed Frequency Domain ICA (FD-ICA) [28]. For its representation, we define the microphone signal vector at time-frequency bin  $(k, n)$  as

$$\underline{\mathbf{x}}(k, n) = [\underline{x}_1(k, n), \dots, \underline{x}_P(k, n)]^T \in \mathbb{C}^P \quad (3)$$

and the corresponding vector of demixed signals as

$$\underline{\mathbf{y}}(k, n) = [\underline{y}_1(k, n), \dots, \underline{y}_P(k, n)]^T \in \mathbb{C}^P. \quad (4)$$

The demixing operation is applied to each frequency bin  $k$  and time frame  $n$  individually and independently

$$\underbrace{\begin{bmatrix} \underline{y}_1(k, n) \\ \vdots \\ \underline{y}_P(k, n) \end{bmatrix}}_{\underline{\mathbf{y}}(k, n)} = \underbrace{\begin{bmatrix} \underline{w}_{11}(k) & \dots & \underline{w}_{P1}(k) \\ \vdots & \ddots & \vdots \\ \underline{w}_{1P}(k) & \dots & \underline{w}_{PP}(k) \end{bmatrix}}_{\check{\mathbf{W}}(k)} \underbrace{\begin{bmatrix} \underline{x}_1(k, n) \\ \vdots \\ \underline{x}_P(k, n) \end{bmatrix}}_{\underline{\mathbf{x}}(k, n)}. \quad (5)$$

Note that  $\check{\mathbf{W}}(k) \in \mathbb{C}^{P \times P}$  contains generally complex-valued scalar elements  $\underline{w}_{pq}(k)$ ,  $p, q \in \{1, \dots, P\}$ , i.e.,  $\check{\mathbf{W}}(k)$  represents instantaneous demixing. The relation between the PDF of the input signal vector  $\underline{\mathbf{x}}(k, n)$  and the output signal vector  $\underline{\mathbf{y}}(k, n)$  can be represented as a linear mapping of complex-valued random variables using (5) [29]

$$p(\underline{\mathbf{y}}(k, n)) = \frac{1}{|\det \check{\mathbf{W}}(k)|^2} p(\underline{\mathbf{x}}(k, n)). \quad (6)$$

Using (6), the cost function for frequency bin  $k$  reflecting the mutual information can be written in terms of the Kullback-Leibler divergence of the observed joint PDF from the ideally separated and thus independent signals as [30]

$$\tilde{J}_{\text{FD-ICA}}(\check{\mathbf{W}}(k)) = \mathcal{KL} \left\{ p(\underline{\mathbf{y}}(k, n)) \left\| \prod_{q=1}^P p(\underline{y}_q(k, n)) \right. \right\} \quad (7)$$

$$= \underbrace{-\mathcal{H}_{p(\underline{\mathbf{x}}(k, n))}}_{\text{const.}} - \sum_{q=1}^P \mathcal{E}_{\text{frame}} \left[ \log p(\underline{y}_q(k)) \right] \dots \dots - 2 \log |\det \check{\mathbf{W}}(k)|, \quad (8)$$

where  $\mathcal{H}_{p(\underline{\mathbf{x}}(k, n))}$  denotes the differential entropy of  $p(\underline{\mathbf{x}}(k, n))$ , which does not depend on the demixing matrix  $\check{\mathbf{W}}(k)$ . The expectation operator is denoted by  $\mathcal{E}_{\text{frame}}$ , where the subscript emphasizes that a statistic over log likelihood values of signal frames has to be estimated. Note that in FD-ICA independent cost functions are used for each frequency bin. After neglecting the constant term and by approximating the expectation operator  $\mathcal{E}_{\text{frame}}[\cdot]$  by arithmetic averaging over all available  $N$  time frames, we obtain as the simplified FD-ICA cost function [28]

$$J_{\text{FD-ICA}}(\check{\mathbf{W}}(k)) := -\frac{1}{N} \sum_{n=0}^{N-1} \left\{ \sum_{q=1}^P \log p(\underline{y}_q(k, n)) \right\} - 2 \log |\det \check{\mathbf{W}}(k)|. \quad (9)$$

Minimizing the FD-ICA cost function (9) decreases the differential entropy of the output signals in each frequency bin, i.e., decreases their Gaussianity, which is expressed by the first term in (9). As a signal mixture is more Gaussian than its input signals, minimizing Gaussianity reverses the mixing process. The second term in (9) promotes linearly independent demixing vectors, i.e., rows of the demixing matrix  $\check{\mathbf{W}}(k)$ , and, hence, ensures that different output signals are extracted. Also trivial solutions by decreasing the first term of (9) by scaling the output signals by demixing matrices comprising elements of small magnitudes are avoided by the second term in (9). Please refer to [31] for a more detailed discussion of the two terms of the cost function in (9).

### IV. INDEPENDENT VECTOR ANALYSIS

As a particular method to address the above-mentioned internal permutation problem, IVA modifies the cost function of FD-ICA by incorporating statistical coupling between the frequency bins for the respective separated sources as shown below.

The demixing operation in IVA is still applied for each frequency bin  $k$  and time frame  $n$  separately according to (5). In contrast to FD-ICA, we now model the vector capturing all  $K$  frequency bins of the STFT-domain output vector for channel  $q$

$$\underline{\mathbf{y}}_q(n) = \left[ \underline{y}_q(1, n), \dots, \underline{y}_q(K, n) \right]^T \in \mathbb{C}^K \quad (10)$$

to follow a  $K$ -variate PDF  $p(\underline{\mathbf{y}}_q(n))$  capturing the statistical dependencies between all frequency bins to avoid the internal permutation problem.

The relation between the PDF of the input signal vectors of all frequency bins  $\underline{\mathbf{x}}(k, n)$ ,  $\forall k$  and the output signal vectors  $\underline{\mathbf{y}}_q(k, n)$ ,  $\forall k$  can - analogously to (6) - be represented by a linear mapping of complex-valued random variables using (5) [29]

$$p(\underline{\mathbf{y}}(1, n), \dots, \underline{\mathbf{y}}(K, n)) = \frac{1}{\left| \prod_{k=1}^K \det \check{\mathbf{W}}(k) \right|^2} p(\underline{\mathbf{x}}(1, n), \dots, \underline{\mathbf{x}}(K, n)). \quad (11)$$

Note that the scaling term stems from the determinant of a  $KQ \times KQ$  block diagonal matrix with  $\check{\mathbf{W}}(k)$  on its block diagonal, see (47) and the illustration in Fig. 4 on the left. The IVA cost function reflecting minimum mutual information can then again be written in terms of the Kullback-Leibler divergence for frequency bin  $k$  as

$$\begin{aligned} \tilde{J}_{\text{IVA}}(\check{\mathbf{W}}(1), \dots, \check{\mathbf{W}}(K)) &= \quad (12) \\ &= \mathcal{KL} \left\{ p(\underline{\mathbf{y}}(1, n), \dots, \underline{\mathbf{y}}(K, n)) \middle| \middle| \prod_{q=1}^P p(\underline{\mathbf{y}}_q) \right\} \\ &= - \underbrace{\mathcal{H}_{p(\underline{\mathbf{x}}(1, n), \dots, \underline{\mathbf{x}}(K, n))}}_{\text{const.}} - \sum_{q=1}^P \mathcal{E}_{\text{frame}} \left[ \log p(\underline{\mathbf{y}}_q) \right] \dots \\ &\quad \dots - 2 \sum_{k=1}^K \log \left| \det \check{\mathbf{W}}(k) \right|, \end{aligned}$$

where  $\mathcal{H}_{p(\underline{\mathbf{x}}(1, n), \dots, \underline{\mathbf{x}}(K, n))}$  denotes the differential entropy of  $p(\underline{\mathbf{x}})$  which is constant w.r.t. the demixing matrices  $\check{\mathbf{W}}(k)$ ,  $k \in \{1, \dots, K\}$ . After neglecting the constant term and by approximating the expectation operator  $\mathcal{E}_{\text{frame}}[\cdot]$  by arithmetic averaging over all  $N$  available time frames, we obtain the cost function [28]

$$\begin{aligned} J_{\text{IVA}}(\check{\mathbf{W}}(1), \dots, \check{\mathbf{W}}(K)) &:= \quad (13) \\ &\sum_{q=1}^P \frac{1}{N} \sum_{n=0}^{N-1} \left\{ -\log p(\underline{\mathbf{y}}_q(n)) \right\} - 2 \sum_{k=1}^K \log \left| \det \check{\mathbf{W}}(k) \right| \end{aligned}$$

depending on all frequency bins  $k$ . We note as the obvious difference to ICA that by using a multivariate source prior, the cost function for each frequency bin  $k$  takes all other frequency bins of all output channels and the demixing systems into account.

Considering (13) and assuming statistical independence between individual frequency bins

$$p(\underline{\mathbf{y}}_q(n)) = \prod_{k=1}^K p(\underline{y}_q(k, n)), \quad (14)$$

we directly obtain independent cost functions per frequency bin. This directly leads to (9) and confirms that FD-ICA is a special case of IVA [28].

## V. TRINICON

As an alternative approach to broadband convolutive BSS, we briefly review the generic TRINICON framework for blind MIMO signal processing, before we establish the link to FD-ICA and IVA. The TRINICON cost function is, in contrast to the previously discussed approaches, defined in the time domain. Therefore, we define the time-domain microphone signal vector with block processing rate  $R$ , i.e., relative shift between two processed frames<sup>2</sup>,

$$\mathbf{x}_p(n) = [x_p(nR), \dots, x_p(nR - 2L + 1)]^T \in \mathbb{R}^{2L} \quad (15)$$

and the time-domain vector of demixed signals

$$\mathbf{y}_q(n) = [y_q(nR), \dots, y_q(nR - D + 1)]^T \in \mathbb{R}^D. \quad (16)$$

The relation between the microphone signals and the demixed signals is modeled by a linear convolution

$$\underbrace{\begin{bmatrix} \mathbf{y}_1(n) \\ \vdots \\ \mathbf{y}_P(n) \end{bmatrix}}_{\mathbf{y}(n)} = \underbrace{\begin{bmatrix} \mathbf{W}_{11} & \dots & \mathbf{W}_{1P} \\ \vdots & \ddots & \vdots \\ \mathbf{W}_{P1} & \dots & \mathbf{W}_{PP} \end{bmatrix}^T}_{\mathbf{W}^T} \underbrace{\begin{bmatrix} \mathbf{x}_1(n) \\ \vdots \\ \mathbf{x}_P(n) \end{bmatrix}}_{\mathbf{x}(n)} \quad (17)$$

with the  $2L \times D$  convolution matrix of Toeplitz structure [24]

$$\mathbf{W}_{pq} = \begin{bmatrix} w_{pq,0} & 0 & \dots & 0 \\ w_{pq,1} & w_{pq,0} & \ddots & \vdots \\ \vdots & w_{pq,1} & \ddots & 0 \\ w_{pq,L-1} & \vdots & \ddots & w_{pq,0} \\ 0 & w_{pq,L-1} & \ddots & w_{pq,1} \\ \vdots & & \ddots & \vdots \\ 0 & \dots & 0 & w_{pq,L-1} \\ 0 & \dots & 0 & 0 \\ \vdots & \dots & \vdots & \vdots \\ 0 & \dots & 0 & 0 \end{bmatrix}. \quad (18)$$

To show the similarities in the derivation compared to FD-ICA and IVA, we will discuss the crucial steps in the derivation of the TRINICON cost function [24], [32]. To this end, we have to perform a change of variables corresponding to (6) and (11), which includes the calculation of the determinant of the demixing matrix. Unfortunately,  $\mathbf{W}$  is not quadratic as the submatrices  $\mathbf{W}_{pq}$  are not quadratic, so that the determinant

<sup>2</sup>Note that  $\mathbf{x}_p(n)$  contains  $2L$  samples instead of  $L + D - 1$  samples required for linear convolution due to consistency with the literature, where this choice is made for deriving concise STFT-domain formulations [24].

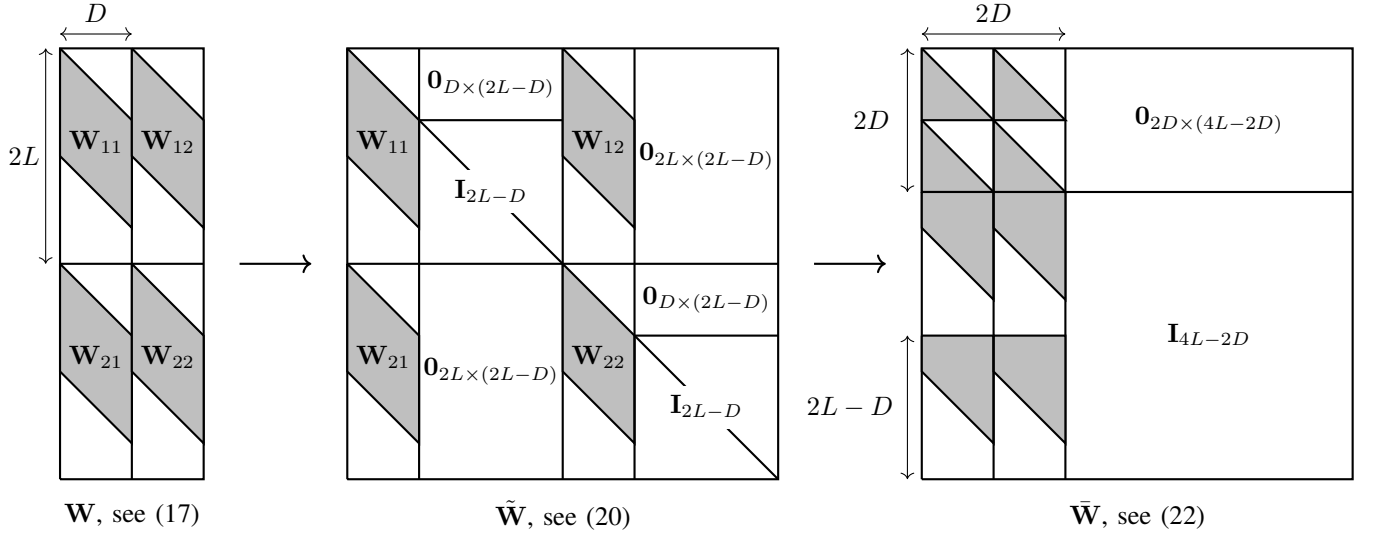


Fig. 2. Extension of the demixing filter matrix  $\mathbf{W}$  of TRINICON for the case  $P = 2$  (cf. [24, Figure B.1]). On the left, the Toeplitz matrix  $\mathbf{W}$  is depicted, which is extended to the matrix  $\tilde{\mathbf{W}}$  by inserting identity matrices  $\mathbf{I}_{2L-D}$  and all-zero matrices, which is shown in the middle. Permutation of rows and columns yields the matrix on the right, which is used to calculate the determinant of the extended demixing filter matrix  $\bar{\mathbf{W}}$ .

does not exist (see Fig. 2, left). Therefore, to facilitate the change of variables, we append the last  $2L - D$  elements of the microphone signals, denoted as  $\tilde{\mathbf{x}}_j(n)$ , to the demixed signals and extend the demixing filter matrix to  $\tilde{\mathbf{W}}$  (see Fig. 2, center), which yields

$$[\mathbf{y}_1^T(n), \tilde{\mathbf{x}}_1^T(n), \dots, \mathbf{y}_P^T(n), \tilde{\mathbf{x}}_P^T(n)]^T = \tilde{\mathbf{W}}^T \mathbf{x}(n). \quad (19)$$

The extended demixing filter matrix yields correspondingly

$$\tilde{\mathbf{W}} = \begin{bmatrix} \mathbf{W}_{11} & \begin{bmatrix} \mathbf{0}_{D \times 2L-D} \\ \mathbf{I}_{2L-D} \end{bmatrix} & \dots & \mathbf{W}_{1P} & \mathbf{0}_{2L \times 2L-D} \\ \vdots & & \ddots & & \vdots \\ \mathbf{W}_{P1} & \mathbf{0}_{2L \times 2L-D} & \dots & \mathbf{W}_{PP} & \begin{bmatrix} \mathbf{0}_{D \times 2L-D} \\ \mathbf{I}_{2L-D} \end{bmatrix} \end{bmatrix}. \quad (20)$$

In the following, we assume that  $\tilde{\mathbf{W}}$  has full rank. Now, we use the rule for a linear mapping of real-valued random vectors of different length [33], i.e., we perform a linear mapping of variables by (20) with subsequent marginalization

$$p(\mathbf{y}(n)) = \frac{1}{|\det \tilde{\mathbf{W}}|} \int_{-\infty}^{\infty} \dots \int_{-\infty}^{\infty} p(\mathbf{x}(n)) d\tilde{\mathbf{x}}_1(n) \dots d\tilde{\mathbf{x}}_P(n). \quad (21)$$

Note that we can use in this case a transformation rule for real-valued random vectors as we operate in time domain compared to FD-ICA and IVA, which operate in the STFT domain.

We rearrange the rows and columns of the extended demixing matrix  $\tilde{\mathbf{W}}$  by applying the permutation matrices  $\mathbf{P}_1$  and

$\mathbf{P}_2$ , to obtain the following permuted extended demixing matrix (see Fig. 2, right)

$$\bar{\mathbf{W}} = \mathbf{P}_1 \tilde{\mathbf{W}} \mathbf{P}_2 = \begin{bmatrix} (\mathbf{U}_{2PL \times PD}^{1D0})^T \mathbf{W} & \mathbf{0}_{PD \times (2PL-PD)} \\ (\mathbf{U}_{2PL \times PD}^{01_{2L-D}})^T \mathbf{W} & \mathbf{I}_{2PL-PD} \end{bmatrix}. \quad (22)$$

Hereby, we defined the following window matrices using the Kronecker product  $\otimes$

$$\mathbf{U}_{2PL \times PD}^{1D0} = \mathbf{I}_P \otimes \begin{bmatrix} \mathbf{I}_D \\ \mathbf{0}_{(2L-D) \times D} \end{bmatrix} \quad (23)$$

and

$$\mathbf{U}_{2PL \times PD}^{01_{2L-D}} = \mathbf{I}_P \otimes \begin{bmatrix} \mathbf{0}_{D \times (2L-D)} \\ \mathbf{I}_{(2L-D)} \end{bmatrix} \quad (24)$$

The application of the permutation matrices does not change the absolute value of the determinant of  $\tilde{\mathbf{W}}$ , i.e.,

$$|\det \tilde{\mathbf{W}}| = |\det \mathbf{P}_1| |\det \tilde{\mathbf{W}}| |\det \mathbf{P}_2| = |\det \bar{\mathbf{W}}|, \quad (25)$$

due to  $|\det \mathbf{P}_1| = |\det \mathbf{P}_2| = 1$  [34]. Furthermore, we observe that  $\bar{\mathbf{W}}$  is a lower block-triangular matrix. Hence, its determinant is given as [34]

$$|\det \bar{\mathbf{W}}| = \left| \det (\mathbf{U}_{2PL \times PD}^{1D0})^T \mathbf{W} \right| |\det \mathbf{I}_{2PL-PD}| = \left| \det (\mathbf{U}_{2PL \times PD}^{1D0})^T \mathbf{W} \right|. \quad (26)$$

Thus, we can conclude that the determinants of the extended demixing matrix  $\tilde{\mathbf{W}}$  and a channel-wise truncated version of the Toeplitz matrices  $(\mathbf{U}_{2PL \times PD}^{1D0})^T \mathbf{W}$  are identical (see Fig. 2) and by evaluating the integral (21) we finally arrive at

$$p(\mathbf{y}(n)) = \frac{1}{\left| \det (\mathbf{U}_{2PL \times PD}^{1D0})^T \mathbf{W} \right|} p(\tilde{\mathbf{x}}(n)), \quad (27)$$

with the shortened vector of microphone signals

$$\bar{\mathbf{x}}(n) = [\bar{\mathbf{x}}_1^T(n), \dots, \bar{\mathbf{x}}_P^T(n)]^T \in \mathbb{R}^{PD}, \quad (28)$$

where each element is defined as

$$\bar{\mathbf{x}}_p(n) = [x_p(nR), \dots, x_p(nR - D + 1)]^T \in \mathbb{R}^D \quad (29)$$

and thus comprises only  $D < 2L$  input samples rather than  $2L$  as in (15). This is due to the marginalization in (21), i.e., the influence of the microphone signal components  $\bar{\mathbf{x}}_p(n)$  is absorbed in the PDF  $p(\bar{\mathbf{x}}(n))$ . Hence, for the statistical properties of the demixed signals expressed by the PDF  $p(\mathbf{y}(n))$  only a dependence on the  $D$  most recent input samples  $\bar{\mathbf{x}}(n)$  is modeled by (27). Thereby, the temporal context of the demixed signals and the observed signals is chosen to be equal. Note that for this line of arguments, only the statistical properties of observed signals and demixed signals are related to each other not the signals themselves, i.e., by applying the demixing matrix as in (17) the actual vector of demixed signals  $\mathbf{y}(n) \in \mathbb{R}^{PD}$  depends on all  $2LP$  samples of the observed signal vector  $\mathbf{x}(n)$ .

The TRINICON BSS cost function is defined as [24]

$$\check{J}_{\text{TRI}}(n', \mathbf{W}) = \sum_{n=0}^{\infty} \beta(n, n') \mathcal{KL} \left\{ p(\mathbf{y}(n)) \left\| \prod_{q=1}^P p(\mathbf{y}_q(n)) \right. \right\}, \quad (30)$$

where  $\beta(n, n')$  is a weighting function controlling the influence of block  $n$  on the cost function evaluated for block  $n'$  and allowing for different versions of the algorithm. The second part of the cost function is the Kullback-Leibler divergence.

The previously discussed algorithms are offline algorithms, i.e., they operate on the complete recorded signal. Therefore, we choose the weighting function  $\beta(n, n')$  to represent the offline version of the TRINICON BSS cost function [24, Section 3.5.1] for comparison

$$\beta(n, n') := \begin{cases} \frac{1}{N} & \text{for } n' \in \{1, \dots, N\} \\ 0 & \text{otherwise} \end{cases}. \quad (31)$$

Insertion of this choice of  $\beta$  into the TRINICON cost function (30) yields

$$\begin{aligned} \check{J}_{\text{TRI}}(\mathbf{W}) &= \frac{1}{N} \sum_{n=0}^{N-1} \mathcal{KL} \left\{ p(\mathbf{y}(n)) \left\| \prod_{q=1}^P p(\mathbf{y}_q(n)) \right. \right\} \\ &= - \underbrace{\mathcal{H}_{p(\bar{\mathbf{x}}(1), \dots, \bar{\mathbf{x}}(N))}}_{\text{const.}} - \frac{1}{N} \sum_{n=0}^{N-1} \sum_{q=1}^P \mathcal{E}_{\text{sample}} [\log p(\mathbf{y}_q(n))] \\ &\quad \dots - \log \left| \det \left( \mathbf{U}_{2PL \times PD}^{1D0} \right)^T \mathbf{W} \right|, \end{aligned} \quad (32)$$

where we used (27) for the change of variables. Note that, analogously to the cost function of FD-ICA (9) and IVA (13) an arithmetic average over all available  $N$  signal blocks is introduced in (32) but also an additional expectation  $\mathcal{E}_{\text{sample}}[\cdot]$  over the log likelihood for subsequent samples of the demixed signals is introduced. Note also that the likelihood functions for FD-ICA, IVA and TRINICON are different in general.

The cost function with approximation of the Kullback-Leibler divergence by sample-wise averaging along the time

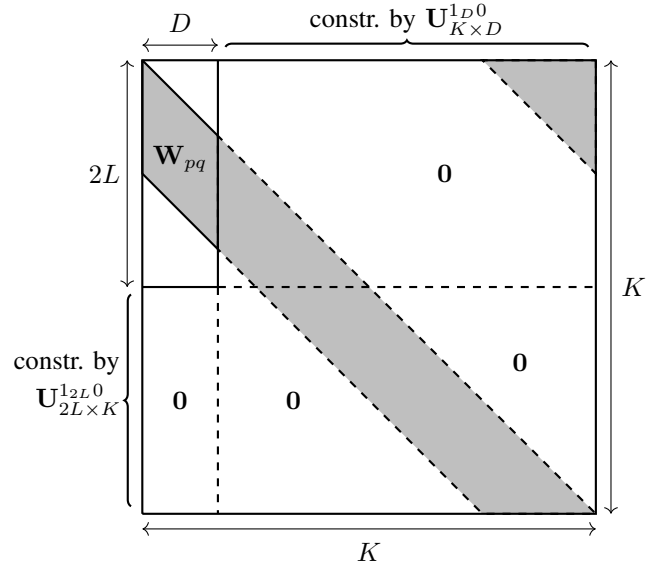


Fig. 3. Extension of a subblock  $\mathbf{W}_{pq}$  of the demixing filter matrix  $\mathbf{W}$  to a circular matrix  $\mathbf{C}_{\mathbf{W}_{pq}}$ . This is accomplished by adding repeating elements until the matrix is a square matrix. Window matrices constrain the obtained circular matrix such that the original Toeplitz matrix can be reconstructed.

axis for each channel  $q$  according to (30), including offline weight and neglecting constant terms yields

$$\begin{aligned} J_{\text{TRI}}(\mathbf{W}) &:= \frac{1}{N} \sum_{n=0}^{N-1} \sum_{q=1}^P \hat{\mathcal{E}}_{\text{sample}} \{-\log p(\mathbf{y}_q(n))\} \dots \\ &\quad + \log \left| \det \left( \mathbf{U}_{2PL \times PD}^{1D0} \right)^T \mathbf{W} \right|. \end{aligned} \quad (33)$$

The last term of (33) can be written explicitly as

$$\begin{aligned} \left( \mathbf{U}_{2PL \times PD}^{1D0} \right)^T \mathbf{W} &= \left( \mathbf{I}_P \otimes \left( \mathbf{U}_{2L \times D}^{1D0} \right)^T \right) \mathbf{W} \\ &= \begin{bmatrix} \left( \mathbf{U}_{2L \times D}^{1D0} \right)^T \mathbf{W}_{11} & \dots & \left( \mathbf{U}_{2L \times D}^{1D0} \right)^T \mathbf{W}_{1P} \\ \vdots & \ddots & \vdots \\ \left( \mathbf{U}_{2L \times D}^{1D0} \right)^T \mathbf{W}_{P1} & \dots & \left( \mathbf{U}_{2L \times D}^{1D0} \right)^T \mathbf{W}_{PP} \end{bmatrix}. \end{aligned} \quad (34)$$

Hence, the matrices  $\mathbf{U}_{2L \times D}^{1D0}$  extract the upper parts of the demixing filter matrices  $\mathbf{W}_{pq}$  (see also Fig. 2 for an illustration). A detailed analysis of the different influence of the log det regularization terms of IVA and TRINICON can be found in [31].

## VI. RELATIONS BETWEEN BSS ALGORITHMS

In the previous sections, we demonstrated that the cost functions of the considered BSS algorithms FD-ICA, IVA and TRINICON follow comparable ideas and we exposed different models underlying the different versions of the Kullback-Leibler divergence as the general cost function.

For a deeper insight into the underlying model assumptions, we want to investigate the relations between the BSS algorithms more closely in the following. To this end, we reformulate the TRINICON and the IVA cost functions, respectively, to obtain representations which allow their analytical comparison.

$$\begin{aligned}
 J_{\text{TRI-FD}}(\mathbf{W}) &= \frac{1}{N} \sum_{n=0}^{N-1} \sum_{q=1}^P \hat{\mathcal{E}}_{\text{sample}} \left\{ -\log p \left( \mathbf{U}_{D \times K}^{1D0} \mathbf{F}_K^{-1} \mathbf{W}_q \mathbf{x}(n) \right) \right\} \\
 &+ \log \left| \det \begin{bmatrix} \mathbf{U}_{D \times K}^{1D0} \mathbf{F}_K \mathbf{W}_{11} \mathbf{F}_K^{-1} (\mathbf{U}_{D \times K}^{1D0})^T & \cdots & \mathbf{U}_{D \times K}^{1D0} \mathbf{F}_K \mathbf{W}_{1P} \mathbf{F}_K^{-1} (\mathbf{U}_{D \times K}^{1D0})^T \\ \vdots & \ddots & \vdots \\ \mathbf{U}_{D \times K}^{1D0} \mathbf{F}_K \mathbf{W}_{P1} \mathbf{F}_K^{-1} (\mathbf{U}_{D \times K}^{1D0})^T & \cdots & \mathbf{U}_{D \times K}^{1D0} \mathbf{F}_K \mathbf{W}_{PP} \mathbf{F}_K^{-1} (\mathbf{U}_{D \times K}^{1D0})^T \end{bmatrix} \right| \\
 &= \frac{1}{N} \sum_{n=0}^{N-1} \hat{\mathcal{E}}_{\text{sample}} \left\{ -\log p \left( \mathbf{U}_{D \times K}^{1D0} \mathbf{F}_K^{-1} \mathbf{W}_q \mathbf{x}(n) \right) \right\} + \log \left| \det \left( \mathbf{I}_P \otimes \mathbf{U}_{D \times K}^{1D0} \mathbf{F}_K \right) \mathbf{W} \left( \mathbf{I}_P \otimes \mathbf{F}_K^{-1} (\mathbf{U}_{D \times K}^{1D0})^T \right) \right|
 \end{aligned} \tag{44}$$

### A. Reformulation of TRINICON

As FD-ICA and IVA are defined in the STFT domain, we will formulate the TRINICON cost function equivalently in the STFT domain.

First, we expand the Toeplitz matrix  $\mathbf{W}_{pq}^T \in \mathbb{R}^{D \times 2L}$  to a circulant matrix  $\mathbf{C}_{\mathbf{W}_{pq}} \in \mathbb{R}^{K \times K}$  with  $K \geq 2L$  and  $L \geq D$  by appending repeating elements to the Toeplitz matrix, see also [22] and Fig. 3

$$\mathbf{W}_{pq}^T = \mathbf{U}_{D \times K}^{1D0} \mathbf{C}_{\mathbf{W}_{pq}} \mathbf{U}_{K \times 2L}^{12L0} \tag{35}$$

where the window matrices

$$\mathbf{U}_{D \times K}^{1D0} = [\mathbf{I}_D \quad \mathbf{0}_{D \times (K-D)}] \tag{36}$$

and

$$\mathbf{U}_{K \times 2L}^{12L0} = \begin{bmatrix} \mathbf{I}_{2L} \\ \mathbf{0}_{(K-2L) \times 2L} \end{bmatrix} \tag{37}$$

cut out the Toeplitz part from the circulant matrix. Next, we use the property that a Discrete Fourier Transform (DFT) matrix

$$\mathbf{F}_K = \frac{1}{\sqrt{K}} \begin{bmatrix} 1 & 1 & 1 & \cdots & 1 \\ 1 & \omega_K & \omega_K^2 & \cdots & \omega_K^{K-1} \\ 1 & \omega_K^2 & \omega_K^4 & \cdots & \omega_K^{2(K-1)} \\ \vdots & \vdots & \vdots & \ddots & \vdots \\ 1 & \omega_K^{K-1} & \omega_K^{2(K-1)} & \cdots & \omega_K^{(K-1)(K-1)} \end{bmatrix}, \tag{38}$$

with  $\omega_K = \exp\left(\frac{-j2\pi}{K}\right)$ , diagonalizes any circulant matrix of corresponding dimensions [35]

$$\mathbf{W}_{pq} = \mathbf{F}_K \mathbf{C}_{\mathbf{W}_{pq}} \mathbf{F}_K^{-1} \tag{39}$$

or equivalently

$$\mathbf{C}_{\mathbf{W}_{pq}} = \mathbf{F}_K^{-1} \mathbf{W}_{pq} \mathbf{F}_K. \tag{40}$$

Hereby, the diagonal matrix  $\mathbf{W}_{pq} \in \mathbb{C}^{K \times K}$  denotes the STFT-domain representation of (18).

By inserting (40) into (35), we obtain for a submatrix of the time-domain demixing filter matrix (see Fig. 3 for an illustration)

$$\begin{aligned}
 \mathbf{W}_{pq} &= (\mathbf{U}_{K \times 2L}^{12L0})^T \mathbf{F}_K \mathbf{W}_{pq} \mathbf{F}_K^{-1} (\mathbf{U}_{D \times K}^{1D0})^T \\
 &= \mathbf{U}_{2L \times K}^{12L0} \mathbf{F}_K \mathbf{W}_{pq} \mathbf{F}_K^{-1} \mathbf{U}_{K \times D}^{1D0}.
 \end{aligned} \tag{41}$$

Now, the output signal  $q$  can be written as

$$\begin{aligned}
 \mathbf{y}_q(n) &= \sum_{p=1}^P \mathbf{W}_{pq}^T \mathbf{x}_p(n) \\
 &= \sum_{p=1}^P \mathbf{U}_{D \times K}^{1D0} \mathbf{F}_K^{-1} \mathbf{W}_{pq} \mathbf{F}_K \mathbf{U}_{K \times 2L}^{12L0} \mathbf{x}_p(n)
 \end{aligned} \tag{42}$$

The STFT representation of the microphone signals, padded with  $K - 2L$  zeros is obtained as

$$\mathbf{x}_p(n) = \mathbf{F}_K [\mathbf{x}_p^T(n) \quad \mathbf{0}_{1 \times (K-2L)}]^T = \mathbf{F}_K \mathbf{U}_{K \times 2L}^{12L0} \mathbf{x}_p. \tag{43}$$

Note that this step ensures the realization of linear convolution instead of circular convolution. Identifying the STFT representation of the microphone signals in (42) yields

$$\begin{aligned}
 \mathbf{y}_q(n) &= \sum_{p=1}^P \mathbf{U}_{D \times K}^{1D0} \mathbf{F}_K^{-1} \mathbf{W}_{pq} \mathbf{x}_p(n) \\
 &= \mathbf{U}_{D \times K}^{1D0} \mathbf{F}_K^{-1} [\mathbf{W}_{1q}, \dots, \mathbf{W}_{Pq}] \underbrace{\begin{bmatrix} \mathbf{x}_1(n) \\ \vdots \\ \mathbf{x}_P(n) \end{bmatrix}}_{\mathbf{x}(n)} \\
 &= \mathbf{U}_{D \times K}^{1D0} \mathbf{F}_K^{-1} \mathbf{W}_q \mathbf{x}(n).
 \end{aligned} \tag{44}$$

We note that the multiplication of the window matrices  $(\mathbf{U}_{2L \times D}^{1D0})^T$  and  $(\mathbf{U}_{K \times 2L}^{12L0})^T$  yields again a window matrix

$$\begin{aligned}
 (\mathbf{U}_{2L \times D}^{1D0})^T (\mathbf{U}_{K \times 2L}^{12L0})^T &= \begin{bmatrix} \mathbf{I}_D \\ \mathbf{0}_{(2L-D) \times D} \end{bmatrix}^T \begin{bmatrix} \mathbf{I}_{2L} \\ \mathbf{0}_{(K-2L) \times 2L} \end{bmatrix}^T \\
 &= \mathbf{U}_{D \times K}^{1D0}.
 \end{aligned} \tag{45}$$

Using this result, we formulate the TRINICON cost function (30) equivalently in the STFT domain by (44).

### B. Reformulation of IVA

In the following section, we will transform the IVA cost function into a representation, which allows a direct comparison with the TRINICON cost function represented in the STFT domain (44).

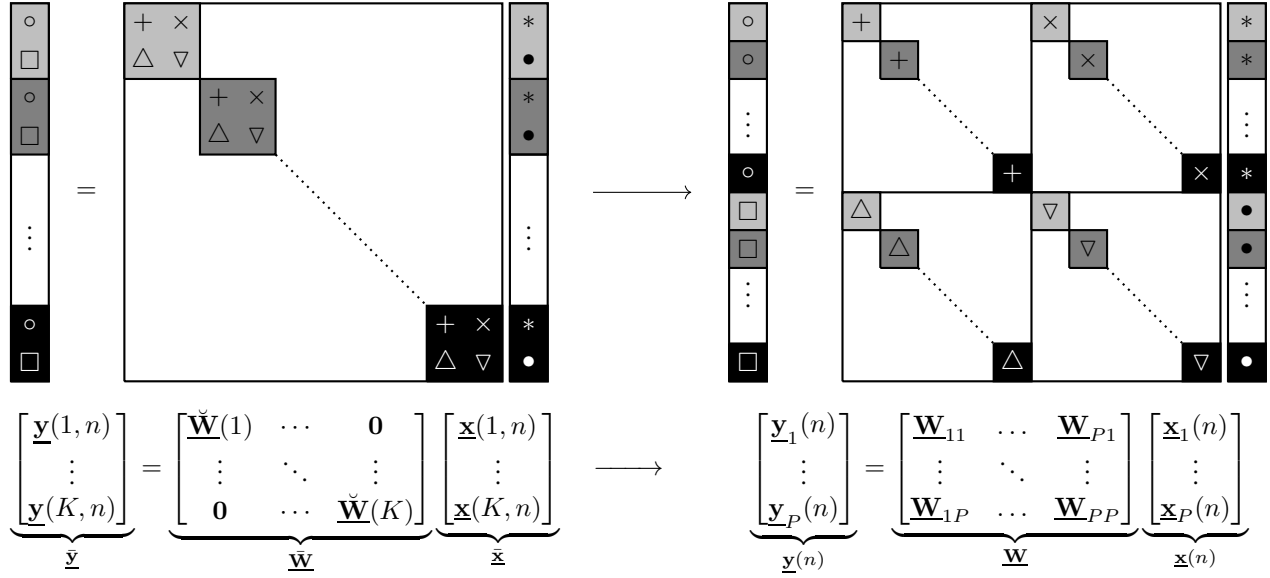


Fig. 4. Illustration of the permutation in the IVA demixing process. The left rectangle in both pictures represents the demixed signal vector, the square the demixing matrix and the right rectangle the microphone vector for an example of 2 sources and 2 channels. Different symbols represent different matrix/vector elements and different gray scales represent different frequencies. The corresponding equations (47) and (53) are shown below the corresponding illustration.

First, we observe that the demixing operation of IVA (and also FD-ICA) can be described by combining (5) for all  $k \in \{1, \dots, K\}$

$$\begin{bmatrix} \underline{\mathbf{y}}(1, n) \\ \vdots \\ \underline{\mathbf{y}}(K, n) \end{bmatrix} = \begin{bmatrix} \check{\mathbf{W}}(1) & \cdots & \mathbf{0} \\ \vdots & \ddots & \vdots \\ \mathbf{0} & \cdots & \check{\mathbf{W}}(K) \end{bmatrix} \begin{bmatrix} \underline{\mathbf{x}}(1, n) \\ \vdots \\ \underline{\mathbf{x}}(K, n) \end{bmatrix}. \quad (47)$$

To obtain the same structure of the demixing operation as for the STFT-domain description of TRINICON, we multiply (47) with a permutation matrix  $\mathbf{P}$  from the left

$$\mathbf{P}\underline{\mathbf{y}} = \mathbf{P}\check{\mathbf{W}}\underline{\mathbf{x}}. \quad (48)$$

Now, we use the fact that permutation matrices are nonsingular and  $\mathbf{P}^{-1} = \mathbf{P}^T$  holds [34]

$$\mathbf{P}\underline{\mathbf{y}} = \mathbf{P}\check{\mathbf{W}}\mathbf{P}^{-1}\mathbf{P}\underline{\mathbf{x}}. \quad (49)$$

The equalities (see (25) for similar calculations)

$$\begin{aligned} \left| \prod_{k=1}^K \det \check{\mathbf{W}}(k) \right| &= |\det \check{\mathbf{W}}| = |\det \mathbf{P} \det \check{\mathbf{W}} \det \mathbf{P}^{-1}| \\ &= |\det \mathbf{P}\check{\mathbf{W}}\mathbf{P}^{-1}| = |\det \mathbf{W}|, \end{aligned} \quad (50)$$

show that the absolute value of the determinant of the demixing matrix does not change when applying the permutation matrices. The rearrangement of the submatrices by the permutation matrices is illustrated in Fig. 4.

The vector of the  $q$ th channel containing all  $K$  frequency bins is defined as

$$\underline{\mathbf{x}}_q(n) = [\underline{x}_q(1, n), \dots, \underline{x}_q(K, n)]^T \quad (51)$$

and the corresponding vector of demixed signals as

$$\underline{\mathbf{y}}_q(n) = [\underline{y}_q(1, n), \dots, \underline{y}_q(K, n)]^T. \quad (52)$$

With these definitions, the demixing process at time frame  $n$  can be written in matrix notation as

$$\begin{bmatrix} \underline{\mathbf{y}}_1(n) \\ \vdots \\ \underline{\mathbf{y}}_P(n) \end{bmatrix} = \begin{bmatrix} \mathbf{W}_{11} & \cdots & \mathbf{W}_{P1} \\ \vdots & \ddots & \vdots \\ \mathbf{W}_{1P} & \cdots & \mathbf{W}_{PP} \end{bmatrix} \begin{bmatrix} \underline{\mathbf{x}}_1(n) \\ \vdots \\ \underline{\mathbf{x}}_P(n) \end{bmatrix} \quad (53)$$

with subblock  $\mathbf{W}_{pq}$  containing all frequency bins defined as

$$\mathbf{W}_{pq} = \begin{bmatrix} w_{pq}(1) & & \mathbf{0} \\ & \ddots & \\ \mathbf{0} & & w_{pq}(K) \end{bmatrix}. \quad (54)$$

The transformation of the PDF of the input signal vector  $\underline{\mathbf{x}}$  to the output signal vector  $\underline{\mathbf{y}}$  is again accomplished by a change of variables

$$p(\underline{\mathbf{y}}(n)) = \frac{1}{|\det \mathbf{W}|^2} p(\underline{\mathbf{x}}(n)). \quad (55)$$

By applying the same rules for a linear mapping of complex-valued random variables, we can show that the PDF of the demixed signals is not affected by the permutation

$$\begin{aligned} p(\underline{\mathbf{y}}(n)) &= p\left(\mathbf{P} [\underline{\mathbf{y}}^T(1, n), \dots, \underline{\mathbf{y}}^T(K, n)]^T\right) \\ &= \frac{1}{|\det \mathbf{P}|^2} p(\underline{\mathbf{y}}(n)) = p(\underline{\mathbf{y}}(n)). \end{aligned} \quad (56)$$

The same holds for  $p(\underline{\mathbf{x}})$ . Hence, we can write the IVA cost function representing the mutual information of the output



channels equivalently as

$$\begin{aligned} \tilde{J}_{\text{IVA}}(\mathbf{W}) &= \mathcal{KL} \left\{ p(\underline{\mathbf{y}}(n)) \left\| \prod_{q=1}^P p(\underline{\mathbf{y}}_q(n)) \right\| \right\} \\ &= \underbrace{\mathcal{H}_{p(\underline{\mathbf{x}}(n))}}_{\text{const.}} - \sum_{q=1}^P \mathcal{E}_{\text{frame}} \left[ \log p(\underline{\mathbf{y}}_q(n)) \right] - 2 \log |\det \mathbf{W}|. \end{aligned} \quad (57)$$

After neglecting constant terms and approximating the expectation operator by averaging over a time interval of  $N$  time-frequency bins along the time axis for each channel  $q$ , we arrive at

$$J_{\text{IVA}}(\mathbf{W}) = \sum_{q=1}^P \frac{1}{N} \sum_{n=0}^{N-1} \left\{ -\log p(\underline{\mathbf{y}}_q(n)) \right\} + 2 \log |\det \mathbf{W}|, \quad (58)$$

or more explicitly at

$$\begin{aligned} J_{\text{IVA}}(\mathbf{W}) &= \sum_{q=1}^P \frac{1}{N} \sum_{n=0}^{N-1} \left\{ -\log p(\mathbf{W}_q \underline{\mathbf{x}}(n)) \right\} \dots \\ &\quad + 2 \log \left| \det \begin{bmatrix} \mathbf{W}_{11} & \dots & \mathbf{W}_{1P} \\ \vdots & \ddots & \vdots \\ \mathbf{W}_{1P} & \dots & \mathbf{W}_{PP} \end{bmatrix} \right|, \end{aligned} \quad (59)$$

where  $\mathbf{W}_q$  represents the  $q$ th row of  $\mathbf{W}$ . Note that (13) and (59) are identical up to the representation of the demixing matrix.

### C. Relation between IVA and TRINICON

In the following, we investigate the relations between the IVA cost function (59) and the TRINICON cost function (44). First of all, in addition to the summation over multiple frames  $n$ , we observe in the TRINICON cost function (44) an expectation over the log-likelihood of output samples in the time domain, which calls for approximation by a sample-wise averaging. This represents the exploitation of nonstationarity of the observations in TRINICON as statistics at different points in time are considered. To simplify the comparison, we eliminate this expectation in the following, i.e., we use instantaneous realizations of the demixed signal vectors. By inspection of (44) and (59), we can furthermore identify two main components in both cost functions: a term reflecting a source model and a log-det term including only the demixing matrix. We compare these two terms individually.

Starting with the source model term, we obtain for TRINICON under the sums over  $n$  and  $q$

$$\log p(\mathbf{U}_{D \times K}^{1D0} \mathbf{F}_K^{-1} \mathbf{W}_q \underline{\mathbf{x}}(n)) \quad (60)$$

and for IVA

$$\log p(\mathbf{W}_q \underline{\mathbf{x}}(n)). \quad (61)$$

By neglecting the window matrix  $\mathbf{U}_{D \times K}^{1D0}$ , i.e., by using a circular convolutive mixture model for TRINICON, both terms are identical up to a DFT. The DFT matrix is a unitary matrix, i.e.,  $|\det \mathbf{F}_K| = 1$ , hence

$$p(\mathbf{F}_K^{-1} \mathbf{W}_q \underline{\mathbf{x}}(n)) = |\det \mathbf{F}_K|^{-2} p(\mathbf{W}_q \underline{\mathbf{x}}(n)) = p(\mathbf{W}_q \underline{\mathbf{x}}(n)). \quad (62)$$

We see that the term corresponding to the source model is equivalent for TRINICON and IVA up to the windowing ensuring the linear convolution model for demixing by TRINICON.

The log-det term reads for TRINICON after removing the window matrices ensuring linear convolution

$$\begin{aligned} &\log |\det (\mathbf{I}_P \otimes \mathbf{F}_K) \mathbf{W} (\mathbf{I}_P \otimes \mathbf{F}_K^{-1})| = \\ &= \log |\det (\mathbf{I}_P \otimes \mathbf{F}_K) \det \mathbf{W} \det (\mathbf{I}_P \otimes \mathbf{F}_K^{-1})| = \\ &= \log |\det (\mathbf{I}_P)^P (\det \mathbf{F}_K)^K \det \mathbf{W} \det (\mathbf{I}_P)^P \det (\mathbf{F}_K^{-1})^K| = \\ &= \log |\det \mathbf{W}|. \end{aligned} \quad (63)$$

Hereby, we used the property that for an  $a \times a$  matrix  $\mathbf{A}$  and a  $b \times b$  matrix  $\mathbf{B}$  the following holds  $\det (\mathbf{A} \otimes \mathbf{B}) = (\det \mathbf{A})^a (\det \mathbf{B})^b$ . The last term in (63) corresponds to the log-det term of the IVA cost function, except for the factor 2. Note that the IVA cost function for real-valued signals does not contain this factor 2 [36] and then exact equality is given.

To summarize, the window matrices ensuring a linear convolution for the demixing system for TRINICON constitute the main difference between TRINICON and IVA. These window matrices disappear for the circular convolution for the demixing system of IVA (see Sec. VI-E for a discussion of its implications). If the window matrices are dropped, the log-det term is essentially the same (up to a factor of 2 stemming from the formulation of IVA in the frequency domain) for IVA and TRINICON. The source terms are also the same when the additional expectation in TRINICON is specialized to instantaneous realizations. IVA can therefore be viewed as a special case of TRINICON resulting from omitting the extra expectation and reducing the linear convolution to a circular one by dropping  $\mathbf{U}_{D \times K}^{1D0}$ .

For IVA, the source model is often specialized to uncorrelated (but not statistically independent frequency bins) [15], which allows to optimize the demixing filter frequency bin-wise. For TRINICON typically correlation between successive signal samples is modeled and, hence, broadband demixing filters are optimized.

### D. Relation Between TRINICON and SOS-based Methods

In the previous section, we showed that the IVA cost function is a special case of the TRINICON cost function up to an additional factor of two originating from the representation of complex-valued random numbers. To this end, we simplified the TRINICON model by relaxation of the linear demixing model to a circulant one and by dropping the exploitation of nonstationarity by an additional expectation over time-domain output samples. In this section, we want to investigate the form of the cost function if the exploitation of nongaussianity is dropped, i.e., only SOS are considered. To this end, we rewrite the TRINICON cost function (32) such that it is expressed as a sum of differential entropies of output signal blocks [30]

$$\begin{aligned} \tilde{J}_{\text{TRI}}(\mathbf{W}) &= \frac{1}{N} \sum_{n=0}^{N-1} \mathcal{KL} \left\{ p(\underline{\mathbf{y}}(n)) \left\| \prod_{q=1}^P p(\underline{\mathbf{y}}_q(n)) \right\| \right\} \\ &= \frac{1}{N} \sum_{n=0}^{N-1} \left( \sum_{q=1}^P \mathcal{H}_{p(\underline{\mathbf{y}}_q(n))} - \mathcal{H}_{p(\underline{\mathbf{y}}(n))} \right). \end{aligned} \quad (64)$$

To express the exclusive dependency on SOS, we choose the output signal vectors to follow a  $PD$ -variate Gaussian distribution

$$\mathbf{y}(n) \sim \mathcal{N}(\mathbf{0}, \mathbf{R}(n)).$$

Due to the statistical independence of the source signals, the covariance matrix of the output signals should be a blockdiagonal matrix, i.e.,

$$\mathbf{R}(n) \stackrel{\dagger}{=} \text{Bdiag}\{\mathbf{R}_1(n), \dots, \mathbf{R}_P(n)\}, \quad (65)$$

where  $\text{Bdiag}\{\cdot\}$  is an operator that generates a block diagonal matrix from its arguments. The  $q$ -th output signal block is  $D$ -variate normally distributed

$$\mathbf{y}_q(n) \sim \mathcal{N}(\mathbf{0}, \mathbf{R}_q(n)). \quad (66)$$

The differential entropies of these Gaussian distributions are given as [30]

$$\mathcal{H}_{p(\mathbf{y}_q(n))} = \frac{1}{2} \log [(2\pi e)^D \det \mathbf{R}_q(n)] \quad (67)$$

$$\mathcal{H}_{p(\mathbf{y}(n))} = \frac{1}{2} \log [(2\pi e)^{PD} \det \mathbf{R}(n)]. \quad (68)$$

Insertion into (64), yields the cost function for SOS TRINICON

$$\begin{aligned} \tilde{J}_{\text{sos}}(\mathbf{W}) &= \frac{PD}{2} \log(2\pi e) \frac{1}{N} \sum_{n=0}^{N-1} \dots \\ &\dots \sum_{q=1}^P \log \det \mathbf{R}_q(n) - \log \det \mathbf{R}(n). \end{aligned} \quad (69)$$

We introduce the  $\text{bdiag}\{\cdot\}$  operator, which sets all block-off-diagonals of the matrix-valued argument to zero, and obtain the following expression, which is proportional to the SOS cost function

$$\tilde{J}_{\text{sos}}(\mathbf{W}) \propto \sum_{n=0}^{N-1} \left\{ \log \det \text{bdiag}\{\mathbf{R}(n)\} - \log \det \mathbf{R}(n) \right\}. \quad (70)$$

This result represents an approximate joint diagonalization problem [37] and coincides with the SOS-based cost function in [22]. It also represents a generalization of a well-known cost function for SOS-based BSS [38, Theorem 1], where the nonstationarity of the (speech) source signals is exploited by considering correlation over multiple time lags by calculating  $D \times D$  correlation matrices (i.e., modeling nonwhiteness) at different time instants  $n$ . While [38] aims at separating instantaneous signal mixtures, (70) deals with convolutive mixtures. However, similar to FD-ICA, convolutive BSS can be addressed by applying instantaneous BSS frequency bin-wise and solving the inner permutation problem. Following this strategy, [38] has been extended to convolutive mixtures in [39]. Similar approaches relying on SOS but employing slightly different cost functions for approximate joint diagonalization in individual frequency bins have been proposed [4], [40], [41].

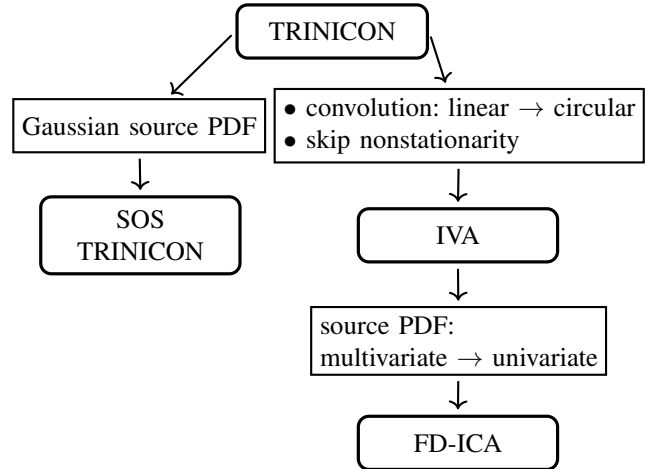


Fig. 5. Illustration of the relations between the discussed BSS algorithms.

### E. Summary - Relation Between Convolutive BSS Algorithms

The relations between the discussed algorithms for convolutive BSS are illustrated in Fig. 5. We showed in Section VI-C that (real-valued) IVA can be considered as a special case of the TRINICON BSS framework. In Section IV, we summarized well-known relations from literature, which state that ICA is a special case of FD-ICA, which is again a special case of IVA. Furthermore, we showed the relation of TRINICON to other SOS-based BSS methods. Hence, TRINICON is shown to be the most general approach of the discussed ICA-based convolutive BSS algorithms.

## VII. IMPACT OF MODEL DIFFERENCES

In this section, we discuss the impact of the identified differences between the algorithms and quantify their influence by experiments.

### A. Exploited Signal Properties and Source Models

For the typical source model applied if IVA is used for audio mixtures, the frequency bins are modeled to follow a supergaussian PDF and to be statistically dependent but uncorrelated [15], i.e., weak-sense nonwhiteness across frequency bins is not taken into account. In FD-ICA, the frequency bins are treated independently, i.e., the frequency bins are assumed to be strictly white and, hence, nonwhiteness is not modeled here either. However, even if weak-sense whiteness is typically assumed for IVA applied to acoustic mixtures [15], [16], the assumption of weak-sense whiteness of the demixed signal vectors is not necessary (see, e.g., [42]), i.e., the demixed signals may be correlated across frequency bins.

Desired acoustic signals are often spectrally structured, i.e., nonwhite, which is ignored by the above-mentioned source models for IVA. Hence, powerful extensions of IVA incorporate models that explicitly model the spectral structure of the source signals. A widely used extension is ILRMA [17] which leverages NMF [43] for modeling frequency-variant

signal variances. The expressive capabilities of deep learning has been exploited for building pre-trained source models for IVA, e.g., [44].

TRINICON is capable to estimate separated sources exploiting multiple source properties and separation is possible even if not all signal properties are fulfilled [24]. It has been shown that modeling of all three signal properties yields faster convergence speed [45] relative to TRINICON variants taking fewer properties into account. However, for TRINICON, non-stationarity can be considered as the most important signal property in terms of a criterion for separation (see [31] for a detailed discussion). FD-ICA and IVA on the other hand, usually rely on nongaussianity if applied to acoustic mixtures and are likely to fail if this signal property is not fulfilled [12].

### B. Ambiguities

The inner permutation problem, i.e., the permutation of the ordering of the output channels among frequency bins, is a well-known problem of, e.g., FD-ICA [28], and has been addressed by numerous repair mechanisms applied as postprocessing step to the separated frequency bins [14], [28]. In contrast, IVA aims at solving this issue directly on cost function level by introducing a multivariate source PDF [15]. However, for auxIVA [16], block permutation effects have been observed [46], i.e., the inner permutation problem is only solved for frequency bins which are close to each other. For distant frequency bins, the statistical coupling is decreased [46] which causes the permutation of frequency blocks. For TRINICON, no inner permutation problems occur as the cost function is defined in time domain, i.e., based on a broadband signal model.

Finally, the so-called filtering ambiguity occurs, i.e., the source signals can only be estimated up to an arbitrary filtering [24]. This is reflected by the fact that TRINICON BSS is estimating the source signals in a filtered (e.g., reverberated version) and does not necessarily equalize (dereverberate) (see [27] for the extension to joint dereverberation and separation). For FD-ICA and IVA, the filtering ambiguity appears as an arbitrary complex (including magnitude and phase) scaling in each frequency bin [28], which has to be addressed prior to transforming the separated signals back to time domain, e.g., by the minimum distortion principle [47]. For implementations of TRINICON, the filtering ambiguity is often addressed by fixing the diagonal filters to represent a pure delay, i.e., by estimating RTFs with the remaining filters [48].

### C. Optimization Strategies

To iteratively minimize the FD-ICA cost function (9), usually a gradient descent algorithm is applied [11]. The gradient update is very often replaced by the natural gradient [49], which generally yields faster convergence due to the fact that the geometric structure of the space of possible solutions is taken into account. Besides gradient-based optimization approaches, also Newton-type algorithms [50] or MM-type algorithms [51] are applied for optimization. A well-known optimization strategy for FD-ICA is the FastICA algorithm

[12] which can be interpreted as a Newton-type optimization method [52].

For minimizing the IVA cost function (13), similar techniques as for FD-ICA have been proposed, e.g., natural gradient [15]. In particular, MM-based optimization algorithms [16], [53]–[56] are used for IVA to separate acoustic sources due to their robust and fast convergence. In addition to that, a fast fixed-point algorithm for IVA has been proposed [57]. The computational complexity of various state-of-the-art optimization approaches for IVA is analyzed in, e.g., [53], [54].

The TRINICON cost function is usually optimized by a steepest descent technique based on the nonholonomic natural gradient [24], [58]. Also a Newton-type algorithm for the optimization of the TRINICON cost function has been proposed [32].

Frequency-domain approaches are known for their lower computational complexity. Hence, the computational load of FD-ICA and IVA can be considered to be lower than a general time-domain implementation of TRINICON. However, several equivalent frequency-domain realizations of TRINICON [22], [24] and real-time strategies based on approximations of the gradient updates [59], [60] have been proposed to compensate for this. The computational complexity of a time-domain real-time implementation of TRINICON is investigated in detail in terms of arithmetic operations in [59].

### D. Convolution Model

Using frequency bin-wise instantaneous BSS, as in FD-ICA and IVA, and transforming the results back into the time domain by inverse STFT corresponds to a circular convolution in the time domain. In contrast, the generic TRINICON cost function constrains the demixing filters (18) to realize a linear convolution. This is expressed by the window matrices  $\mathbf{U}$  in (33) and in its frequency-domain representation (44).

The limitations of the circular convolution model has been extensively studied in literature, e.g., [61], and especially for FD-ICA in, e.g., [2], [62]–[64]. To approximately represent linear convolution, i.e., to limit circular convolution effects, long STFT windows are desirable. However, this reduces the number of available data samples per frequency bin to estimate statistics needed for the BSS algorithm or requires a large degree of overlap of data blocks with accordingly increased computational complexity. As FD-ICA and IVA share the same convolution model, these arguments apply to IVA as well.

Hence, we can conclude that FD-ICA and IVA necessarily need to compromise regarding the approximation of the linear convolution and the capability to estimate desired signal statistics. On the other hand, no such compromise is necessary with TRINICON.

### E. Experiments

For an experimental comparison of the methods which exemplarily illustrates the findings above, we focus on IVA and TRINICON in a determined scenario of  $P = 2$  sources and two microphones and consider only the performance after convergence. A comparison of the separation performance of

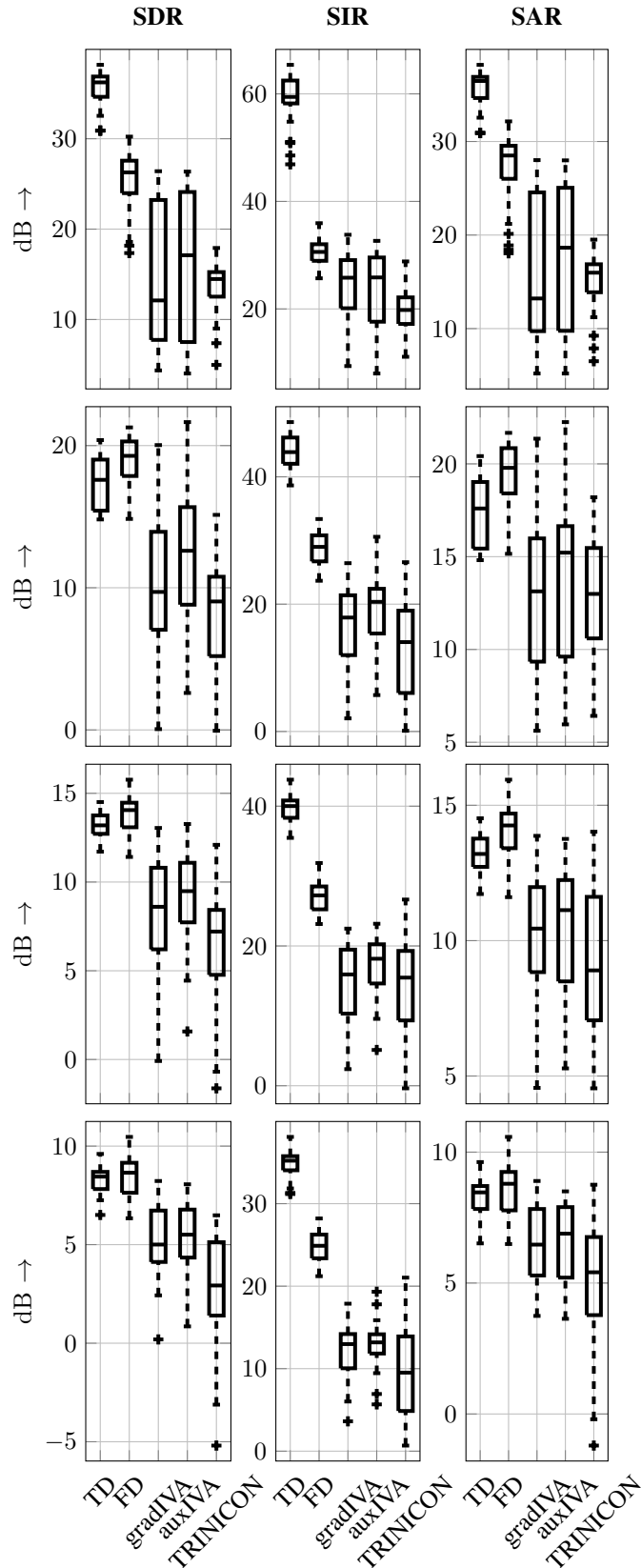


Fig. 6. Results in terms of output SDR, SIR and SAR of the discussed methods. The first row of plots corresponds to the low-reverberant chamber ( $T_{60} = 0.05$  s), the second and third row to the two meeting rooms ( $T_{60} = 0.2$  s and  $T_{60} = 0.4$  s) and the last row to the seminar room ( $T_{60} = 0.9$  s).

FD-ICA and IVA has been presented in [65]. The microphone signals are simulated by (linearly) convolving speech signals randomly chosen from a set of four male and four female speakers of 10 s duration with measured RIRs. To obtain representative results, in each experiment with a fixed acoustic situation, the two speech signals have been drawn 20 times from the set of available clean speech signals. The RIRs were measured with a microphone pair of 4.2 cm spacing from four different rooms: a low-reverberant chamber ( $T_{60} = 0.05$  s), two meeting rooms ( $T_{60} = 0.2$  s and  $T_{60} = 0.4$  s) and a seminar room ( $T_{60} = 0.9$  s). The sources have been placed at 1 m distance from the microphones and at  $\pm 45^\circ$  from broadside direction.

To obtain a benchmark for ideal performance of a demixing system realized by circular and linear convolution, we identified Relative Transfer Functions (RTFs) between the two microphones based on the source images. On one hand, we estimated a relative impulse response as an FIR filter realizing a linear convolution by solving a least squares problem in time domain. This approach is abbreviated as TD. On the other hand we identified an RTF separately in each frequency bin by solving a least squares problem, which represents a circular convolution and is named FD. To compare IVA and TRINICON, we chose natural gradient update schemes [15], [24] and, additionally for IVA, update rules derived from the MM perspective called auxIVA [16]. For IVA, a Laplacian source prior [15], [16] has been used. The exploitation of nongaussianity did not yield a significant benefit in the presented experiments in terms of the steady-state performance of TRINICON and has therefore been dropped, i.e., we used a SOS realization of TRINICON as described in Sec. VI-D. However, as mentioned earlier, exploiting HOS increases – especially initial – convergence speed (see [45]).

The filter length (corresponding to the DFT length for the STFT-based methods) of all approaches has been set to 2048 at a sampling rate of 16 kHz. For IVA we chose a Hamming window with 50% overlap for the STFT transform. With 10 s signal duration and  $f_s = 16$  kHz sampling rate, this leads to  $N = 156$  frames for IVA and  $N = 78$  frames for TRINICON. Furthermore, we used a step size of 0.1 and 1000 for gradient-based IVA (gradIVA) and a step size of 0.005 and 1000 iterations for TRINICON. For auxIVA, we used 100 iterations. These parameters have been identified experimentally and showed good performance on average. The performance of the algorithms has been measured in terms of Signal-to-Distortion Ratio (SDR), Signal-to-Interference Ratio (SIR) and Signal-to-Artifact Ratio (SAR) [65].

Fig. 6 shows the results of the described experiments, where each row corresponds to one of the four considered acoustic enclosures. It can be observed that the oracle approaches TD and FD obtained as expected the best results, where the linear convolutive method TD outperformed FD in terms of SIR. This is to be expected as the linear convolution model is physically more meaningful and follows the experimental setup. Furthermore, the clear superiority in terms of SIR can be understood as the interference suppression was the objective we optimized for. The inferior performance in terms of SDR and SAR for large reverberation times can be at-

tributed to the fact that RTFs may require a longer time-domain representation than the impulse responses itself. For the BSS methods based on the natural gradient, TRINICON and gradIVA obtained for small reverberation times similar performance. At larger reverberation times, TRINICON has been outperformed by gradIVA. This can be explained by the fact that the exploited signal properties are less affected by reverberation in frequency domain than in time domain (see [31] for a detailed analysis). By exploiting the MM principle, auxIVA obtained better results than the gradient-based algorithms in all cases.

Although TRINICON represents a more general cost function and uses a linear convolution model, which has been experimentally shown to be superior over the circular one, the performance after convergence is slightly worse than gradIVA and significantly inferior to auxIVA. Therefore, we conclude that future work should investigate more powerful ways for the optimization of the TRINICON cost function that allow to exploit the generality of the cost function and the benefit of the linear convolution model.

### VIII. CONCLUSION

In this contribution, we provided an in-depth and rigorous analysis of the relation between the cost functions of various convolutive BSS approaches based on ICA. The similarity of the derivation of the considered cost functions has been demonstrated by explicitly performing corresponding calculations. By deriving a common representation for all cost functions, we showed that the TRINICON cost function includes the IVA cost function, which again includes the FD-ICA cost function as special cases. The main differences between the cost function we identified are the linear instead of a circular convolution model and the exploitation of nonstationarity in TRINICON. Furthermore, the relation between the TRINICON cost function and SOS-based methods has been shown. These identified differences are discussed and related to results from the literature. In this sense, we provided a common roof for all of these algorithms allowing the identification of similarities and differences in the underlying models. Finally, experiments using measured RIRs compared the performance of IVA and TRINICON and benchmarked it with oracle demixing matrices based on a linear and a circular convolution model, respectively.

### REFERENCES

- [1] S. Makino, T.-W. Lee, and H. Sawada, Eds., *Blind speech separation*, ser. Signals and communication technology. Dordrecht: Springer, 2007.
- [2] M. S. Pedersen, J. Larsen, U. Kjems, and L. C. Parra, "A Survey of Convolutive Blind Source Separation Methods," in *Springer Handbook of Speech Processing*, J. Benesty, Y. Huang, and M. M. Sondhi, Eds., Nov. 2007.
- [3] T. Mei and F. Yin, "Blind separation of convolutive mixtures by decorrelation," *Signal Processing*, vol. 84, no. 12, pp. 2297–2313, Dec. 2004.
- [4] L. Parra and C. Spence, "Convolutive blind separation of non-stationary sources," *IEEE Transactions on Speech and Audio Processing*, vol. 8, no. 3, pp. 320–327, May 2000.
- [5] E. Weinstein, M. Feder, and A. Oppenheim, "Multi-channel signal separation by decorrelation," *IEEE Transactions on Speech and Audio Processing*, vol. 1, no. 4, pp. 405–413, Oct. 1993.
- [6] R. Aichner, S. Araki, S. Makino, T. Nishikawa, and H. Saruwatari, "Time domain blind source separation of non-stationary convoluted signals by utilizing geometric beamforming," in *Proceedings of the 12th IEEE Workshop on Neural Networks for Signal Processing*, Martigny, Switzerland, 2002, pp. 445–454.
- [7] P. Tichavsky and Z. Koldovský, "Fast and accurate methods for independent component analysis: A survey," *Kybernetika*, vol. 47, no. 3, pp. 426–438, 2011.
- [8] P. Comon, E. Moreau, and L. Rota, "Blind separation of convolutive mixtures: A contrast-based approach," in *ICA'01*, 2001, pp. 686–691.
- [9] W. Baumann, D. Kolossa, and R. Orglmeister, "Beamforming-based convolutive source separation," in *2003 IEEE International Conference on Acoustics, Speech, and Signal Processing, 2003. Proceedings. (ICASSP '03)*, vol. 5, Hong Kong, China, 2003, pp. V–357–60.
- [10] N. Charkani and Y. Deville, "A convolutive source separation method with self-optimizing non-linearities," in *1999 IEEE International Conference on Acoustics, Speech, and Signal Processing. Proceedings. ICASSP99 (Cat. No.99CH36258)*, Phoenix, AZ, USA, 1999, pp. 2909–2912 vol.5.
- [11] A. J. Bell and T. J. Sejnowski, "An Information-Maximization Approach to Blind Separation and Blind Deconvolution," *Neural Computation*, vol. 7, no. 6, pp. 1129–1159, Nov. 1995.
- [12] A. Hyvärinen, J. Karhunen, and E. Oja, *Independent component analysis*. New York: J. Wiley, 2001.
- [13] P. Smaragdis, "Blind Separation of Convoluted Mixtures in the Frequency Domain," *Neurocomputing Journal*, vol. 22, pp. 21–34, 1998.
- [14] H. Sawada, R. Mukai, S. Araki, and S. Makino, "A Robust and Precise Method for Solving the Permutation Problem of Frequency-Domain Blind Source Separation," *IEEE Transactions on Speech and Audio Processing*, vol. 12, no. 5, pp. 530–538, Sep. 2004.
- [15] T. Kim, H. T. Attias, S.-Y. Lee, and T.-W. Lee, "Blind Source Separation Exploiting Higher-Order Frequency Dependencies," *IEEE Transactions on Audio, Speech and Language Processing*, vol. 15, no. 1, pp. 70–79, Jan. 2007.
- [16] N. Ono, "Stable and fast update rules for independent vector analysis based on auxiliary function technique," in *IEEE Workshop Applications Signal Process. to Audio, Acoustics (WASPAA)*, New Paltz, NY, USA, Oct. 2011, pp. 189–192.
- [17] D. Kitamura, N. Ono, H. Sawada, H. Kameoka, and H. Saruwatari, "Determined Blind Source Separation Unifying Independent Vector Analysis and Nonnegative Matrix Factorization," *IEEE/ACM Transactions on Audio, Speech, and Language Processing*, vol. 24, no. 9, pp. 1626–1641, Sep. 2016.
- [18] A. H. Khan, M. Taseska, and E. A. P. Habets, "A Geometrically Constrained Independent Vector Analysis Algorithm for Online Source Extraction," in *Latent Variable Analysis and Signal Separation*, E. Vincent, A. Yeredor, Z. Koldovský, and P. Tichavský, Eds. Cham: Springer International Publishing, 2015, vol. 9237, pp. 396–403.
- [19] A. Brendel, T. Haubner, and W. Kellermann, "Spatially Guided Independent Vector Analysis," in *IEEE International Conference on Acoustics, Speech, and Signal Processing (ICASSP)*, Barcelona, Spain, May 2020.
- [20] —, "A Unified Probabilistic View on Spatially Informed Source Separation and Extraction Based on Independent Vector Analysis," *IEEE Transactions on Signal Processing*, vol. 68, pp. 3545–3558, 2020.
- [21] Z. Koldovsky and P. Tichavsky, "Gradient Algorithms for Complex Non-Gaussian Independent Component/Vector Extraction, Question of Convergence," *IEEE Transactions on Signal Processing*, vol. 67, no. 4, pp. 1050–1064, Feb. 2019.
- [22] H. Buchner, R. Aichner, and W. Kellermann, "A generalization of blind source separation algorithms for convolutive mixtures based on second-order statistics," *IEEE Transactions on Speech and Audio Processing*, vol. 13, no. 1, pp. 120–134, Jan. 2005.
- [23] —, "Blind source separation for convolutive mixtures: A unified treatment," in *Audio Signal Processing for the Next-Generation Multimedia Communication Systems*, J. Benesty and Y. Huang, Eds. Boston: Kluwer Academic Publishers, Apr. 2004, pp. 255–293.
- [24] R. Aichner, "Acoustic Blind Source Separation in Reverberant and Noisy Environments," PHD Thesis, University Erlangen-Nuremberg, 2007.
- [25] A. Lombard, Y. Zheng, H. Buchner, and W. Kellermann, "TDOA Estimation for Multiple Sound Sources in Noisy and Reverberant Environments Using Broadband Independent Component Analysis," *IEEE Transactions on Audio, Speech, and Language Processing*, vol. 19, no. 6, pp. 1490–1503, Aug. 2011.
- [26] K. Reindl, S. Meier, H. Barfuss, and W. Kellermann, "Minimum Mutual Information-Based Linearly Constrained Broadband Signal Extraction," *IEEE/ACM Transactions on Audio, Speech, and Language Processing*, vol. 22, no. 6, pp. 1096–1108, Jun. 2014.

- [27] H. Buchner and W. Kellermann, "TRINICON for Dereverberation of Speech and Audio Signals," in *Speech Dereverberation*, P. Naylor and N. Gaubitch, Eds. Springer, New York, 2010, pp. 311–385.
- [28] E. Vincent, T. Virtanen, and S. Gannot, Eds., *Audio source separation and speech enhancement*. Hoboken, NJ: John Wiley & Sons, 2018.
- [29] E. Moreau and T. Adali, *Blind identification and separation of complex-valued signals*, ser. Focus series in digital signal and image processing. London : Hoboken, NJ: ISTE ; Wiley, 2013.
- [30] T. M. Cover and J. A. Thomas, *Elements of information theory*, 2nd ed. Hoboken, N.J: Wiley-Interscience, 2006.
- [31] A. Brendel, "From Blind to Semi-Blind Acoustic Source Separation based on Independent Component Analysis," PHD Thesis, University Erlangen-Nuremberg, 2022.
- [32] H. Buchner, "Broadband Adaptive MIMO Filtering: A Unified Treatment and Applications to Acoustic Human-Machine Interfaces," PHD Thesis, University Erlangen-Nuremberg, Erlangen, 2010.
- [33] A. Papoulis, *Probability, random variables, and stochastic processes*, 2nd ed., ser. McGraw-Hill series in electrical engineering. New York: McGraw-Hill, 1984.
- [34] D. A. Harville, *Matrix algebra from a statistician's perspective*. New York: Springer, 2008.
- [35] G. H. Golub and C. F. Van Loan, *Matrix computations*, 3rd ed., ser. Johns Hopkins studies in the mathematical sciences. Baltimore: Johns Hopkins University Press, 1996.
- [36] M. Anderson, G.-S. Fu, R. Phlypo, and T. Adali, "Independent Vector Analysis: Identification Conditions and Performance Bounds," *IEEE Transactions on Signal Processing*, vol. 62, no. 17, pp. 4399–4410, Sep. 2014.
- [37] D. T. Pham, "Joint Approximate Diagonalization of Positive Definite Hermitian Matrices," *SIAM Journal on Matrix Analysis and Applications*, vol. 22, no. 4, pp. 1136–1152, 2001.
- [38] K. Matsuoka, M. Ohoya, and M. Kawamoto, "A neural net for blind separation of nonstationary signals," *Neural Networks*, vol. 8, no. 3, pp. 411–419, Jan. 1995.
- [39] N. Murata, S. Ikeda, and A. Ziehe, "An approach to blind source separation based on temporal structure of speech signals," *Neurocomputing*, vol. 41, no. 1–4, pp. 1–24, Oct. 2001.
- [40] M. Ikram and D. Morgan, "Permutation inconsistency in blind speech separation: investigation and solutions," *IEEE Transactions on Speech and Audio Processing*, vol. 13, no. 1, pp. 1–13, Jan. 2005.
- [41] G. Chabriel, M. Kleinstueber, E. Moreau, H. Shen, P. Tichavsky, and A. Yeredor, "Joint Matrices Decompositions and Blind Source Separation: A survey of methods, identification, and applications," *IEEE Signal Processing Magazine*, vol. 31, no. 3, pp. 34–43, May 2014.
- [42] M. Anderson, T. Adali, and X.-L. Li, "Joint Blind Source Separation With Multivariate Gaussian Model: Algorithms and Performance Analysis," *IEEE Transactions on Signal Processing*, vol. 60, no. 4, pp. 1672–1683, Apr. 2012.
- [43] C. Févotte, N. Bertin, and J.-L. Durrieu, "Nonnegative Matrix Factorization with the Itakura-Saito Divergence: With Application to Music Analysis," *Neural Computation*, vol. 21, no. 3, pp. 793–830, Mar. 2009.
- [44] N. Makishima, S. Mogami, N. Takamune, D. Kitamura, H. Sumino, S. Takamichi, H. Saruwatari, and N. Ono, "Independent Deeply Learned Matrix Analysis for Determined Audio Source Separation," *IEEE/ACM Transactions on Audio, Speech, and Language Processing*, vol. 27, no. 10, pp. 1601–1615, Oct. 2019.
- [45] H. Buchner, R. Aichner, and W. Kellermann, "Blind Source Separation for Convolutional Mixtures Exploiting Nongaussianity, Nonwhiteness, and Nonstationarity," in *International Workshop on Acoustic Echo and Noise Control (IWAENC)*, Kyoto, Japan, Sep. 2003.
- [46] Y. Liang, S. Naqvi, and J. Chambers, "Overcoming block permutation problem in frequency domain blind source separation when using AuxIVA algorithm," *Electronics Letters*, vol. 48, no. 8, p. 460, 2012.
- [47] K. Matsuoka, "Minimal distortion principle for blind source separation," vol. 4. Soc. Instrument & Control Eng. (SICE), 2002, pp. 2138–2143.
- [48] S. Meier and W. Kellermann, "Analysis of the performance and limitations of ICA-based relative impulse response identification," in *European Signal Processing Conference (EUSPICO)*, Aug. 2015, pp. 414–418.
- [49] S.-I. Amari, "Natural Gradient Works Efficiently in Learning," vol. 10, no. 2, pp. 251–276, Feb. 1998.
- [50] J. A. Palmer, S. Makeig, K. Kreutz-Delgado, and B. D. Rao, "Newton method for the ICA mixture model," Mar. 2008, pp. 1805–1808.
- [51] N. Ono and S. Miyabe, "Auxiliary-Function-Based Independent Component Analysis for Super-Gaussian Sources," in *Latent Variable Analysis and Signal Separation*, V. Vigneron, V. Zarzoso, E. Moreau, R. Gribonval, and E. Vincent, Eds. Berlin, Heidelberg: Springer Berlin Heidelberg, 2010, vol. 6365, pp. 165–172.
- [52] A. Hyvarinen, "Fast and robust fixed-point algorithms for independent component analysis," *IEEE Transactions on Neural Networks*, vol. 10, no. 3, pp. 626–634, May 1999.
- [53] R. Scheibler and N. Ono, "Fast and Stable Blind Source Separation with Rank-1 Updates," in *ICASSP 2020 - 2020 IEEE International Conference on Acoustics, Speech and Signal Processing (ICASSP)*, Barcelona, Spain, May 2020, pp. 236–240.
- [54] R. Scheibler, "Independent Vector Analysis via Log-Quadratically Penalized Quadratic Minimization," *IEEE Transactions on Signal Processing*, vol. 69, pp. 2509–2524, 2021.
- [55] A. Brendel and W. Kellermann, "Accelerating Auxiliary Function-based Independent Vector Analysis," in *IEEE International Conference on Acoustic, Speech and Signal Processing (ICASSP)*, Toronto, Canada, Jun. 2021, pp. 496–500.
- [56] —, "FasterIVA: Update Rules for Independent Vector Analysis based on Negentropy and the Majorize-Minimize Principle," in *IEEE Workshop on Applications of Signal Processing to Audio and Acoustics (WASPAA)*, New Paltz, USA, Oct. 2021, pp. 131–135.
- [57] I. Lee, T. Kim, and T.-W. Lee, "Fast fixed-point independent vector analysis algorithms for convolutive blind source separation," *Signal Processing*, vol. 87, no. 8, pp. 1859–1871, Aug. 2007.
- [58] S.-I. Amari, T.-P. Chen, and A. Cichocki, "Nonholonomic Orthogonal Learning Algorithms for Blind Source Separation," *Neural Computation*, vol. 12, no. 6, pp. 1463–1484, Jun. 2000.
- [59] R. Aichner, H. Buchner, F. Yan, and W. Kellermann, "A real-time blind source separation scheme and its application to reverberant and noisy acoustic environments," *Signal Processing*, vol. 86, no. 6, pp. 1260–1277, Jun. 2006.
- [60] C. A. Anderson, S. Meier, W. Kellermann, P. D. Teal, and M. A. Poletti, "A GPU-accelerated real-time implementation of TRINICON-BSS for multiple separation units," May 2014, pp. 102–106.
- [61] W. Kellermann and H. Buchner, "Wideband algorithms versus narrow-band algorithms for adaptive filtering in the DFT domain," 2003, pp. 1278–1282.
- [62] S. Araki, R. Mukai, S. Makino, T. Nishikawa, and H. Saruwatari, "The fundamental limitation of frequency domain blind source separation for convolutive mixtures of speech," *IEEE Transactions on Speech and Audio Processing*, vol. 11, no. 2, pp. 109–116, Mar. 2003.
- [63] S. Makino, "Blind Source Separation of Convolutive Mixtures of Speech in Frequency Domain," *IEICE Transactions on Fundamentals of Electronics, Communications and Computer Sciences*, vol. E88-A, no. 7, pp. 1640–1655, Jul. 2005.
- [64] H. Sawada, R. Mukai, S. Araki, and S. Makino, "Convolutive blind source separation for more than two sources in the frequency domain," in *2004 IEEE International Conference on Acoustics, Speech, and Signal Processing*, vol. 3, Montreal, Que., Canada, 2004, pp. iii–885–8.
- [65] E. Vincent, R. Gribonval, and C. Févotte, "Performance measurement in blind audio source separation," *IEEE Transactions on Audio, Speech and Language Processing*, vol. 14, no. 4, pp. 1462–1469, Jul. 2006.